



Published in final edited form as:

Nat Plants. ; 2: 16179. doi:10.1038/nplants.2016.179.

Origin and function of stomata in the moss *Physcomitrella patens*

Caspar C. Chater^{1,‡}, Robert S. Caine^{2,‡}, Marta Tomek³, Simon Wallace⁴, Yasuko Kamisugi⁵, Andrew C. Cuming⁵, Daniel Lang³, Cora A. MacAlister⁶, Stuart Casson⁷, Dominique C. Bergmann⁸, Eva L. Decker³, Wolfgang Frank⁹, Julie E. Gray⁷, Andrew Fleming², Ralf Reski^{3,10,*}, and David J. Beerling^{2,*}

¹Departamento de Biología Molecular de Plantas, Instituto de Biotecnología, Universidad Nacional Autónoma de México, Cuernavaca, México

²Department of Animal and Plant Sciences, University of Sheffield, Sheffield S10 2TN, UK

³Plant Biotechnology, Faculty of Biology, University of Freiburg, Schänzlestr. 1, 79104 Freiburg, Germany

⁴Royal College of Veterinary Surgeons, Belgravia House, 62-64 Horseferry Rd, London SW1P 2AF, UK

⁵Centre for Plant Sciences, University of Leeds, Leeds, LS2 9JT, UK

⁶Department of Molecular Cellular and Developmental Biology, University of Michigan, Ann Arbor, Michigan, 48109-1048, USA

⁷Department of Molecular Biology and Biotechnology, University of Sheffield, Sheffield S10 2TN, UK

⁸HHMI and Department of Biology, Stanford University, Stanford, CA 94305-5020, USA

⁹Plant Molecular Cell Biology, Faculty of Biology, Ludwig-Maximilians-Universität München, LMU Biocenter, Großhaderner Straße 2, 82152 Planegg-Martinsried, Germany

¹⁰BIOSS – Centre for Biological Signalling Studies, 79104 Freiburg, Germany

Abstract

Stomata are microscopic valves on plant surfaces that originated over 400 million years ago and facilitated the greening of Earth's continents by permitting efficient shoot-atmosphere gas

Users may view, print, copy, and download text and data-mine the content in such documents, for the purposes of academic research, subject always to the full Conditions of use: http://www.nature.com/authors/editorial_policies/license.html#terms

*Corresponding authors. d.j.beerling@sheffield.ac.uk, ralf.reski@biologie.uni-freiburg.de.

‡These authors contributed equally to this work.

Author contributions

C.C.C., R.C., R.R., W.F., J.E.G., A.F., D.J.B. and R.R. designed the study, C.C.C., R.C., D.L. and M.T. undertook the experiments with contributions from S.W., Y.K. and A.C.C., C.A.M., S.C., D.C.B., D.L., E.L.D. and W.F. contributed materials and advice. A.C.C. constructed vectors for moss targeted knockout (SMF1 and SMF2), Y.K. carried out moss transformation (SMF2-KO) and yeast-2-hybrid analysis, A.C.C. and Y.K. carried out Southern blot hybridisation of the knockout mutant lines. D.J.B., R.R., C.C.C. and R.C. wrote the paper with contributions from D.C.B. All authors read, commented on and approved the final version of the manuscript.

Availability. All moss mutants described here were deposited in the International Moss Stock Center IMSC (Supplemental Table S2).

exchange and plant hydration¹. However, the core genetic machinery regulating stomatal development in non-vascular land plants is poorly understood^{2–4} and their function has remained a matter of debate for a century⁵. Here, we show that genes encoding the two basic helix-loop-helix proteins PpSMF1 and PpSCRM1 in the moss *Physcomitrella patens* are orthologous to transcriptional regulators of stomatal development in the flowering plant *Arabidopsis thaliana* and essential for stomata formation in moss. Targeted knock-out *P. patens* mutants lacking either *PpSMF1* or *PpSCRM1* develop gametophytes indistinguishable from wild-type plants but mutant sporophytes lacking stomata. Protein-protein interaction assays reveal heterodimerisation between *PpSMF1* and *PpSCRM1* which, together with moss-angiosperm gene complementations⁶, suggests deep functional conservation of the heterodimeric *SMF1* and *SCRM1* unit required to activate transcription for moss stomatal development, as in *A. thaliana*⁷. Moreover, stomata-less sporophytes of *PpSMF1* and *PpSCRM1* mutants exhibited delayed dehiscence, implying stomata might have promoted dehiscence in the first complex land plant sporophytes.

Colonization of terrestrial environments by green plants approximately 500 million years ago (Ma) established the basis for the emergence of complex land-based ecosystems that fundamentally transformed the biogeochemical cycling of carbon, water and energy^{1,8}. Fossils suggest stomata originated on the small leafless sporophytes of the earliest vascular land plants, such as *Cooksonia*, over 410 Ma, and predated the evolutionary appearance of leaves and roots⁹. Insight into the core developmental modules has emerged from studies on the evolution of roots^{10,11}, shoots¹², and land plant life cycles^{13,14}. We know little, however, about the core regulatory genes governing the specialized differentiation of guard cells that formed stomatal pores in basal land plant lineages.

Here, we address the origin of stomata in land plants by elucidating the key genetic components controlling stomatal development in the moss *Physcomitrella patens*. Targeted molecular genetic studies with *P. patens* provide insight into the genetic toolkit adopted by early land plants because stomata evolved in the common ancestor of mosses and vascular plants¹⁵. *P. patens* belongs to an extant basal lineage of non-vascular land plants that develop stomata exclusively on the diploid sporophyte (Figures 1 a–c), although the major photosynthetic moss tissue is the haploid leafy gametophyte. Knowledge of the genetic controls on moss stomatal development is rudimentary². In *Arabidopsis*, a representative of the dicot flowering plants, developmental stages leading to stomatal formation are controlled primarily by the action of three closely related Group Ia basic helix-loop-helix (bHLH) proteins (SPEECHLESS (SPCH), MUTE and FAMA)¹⁶. Each of these three bHLHs regulates a key successive step in stomatal lineage behaviour, and each requires heterodimerisation with either of the more broadly expressed Group IIIb bHLH proteins SCREAM1(SCRM1)/ICE1 or SCRM2^{7,17}. Evolutionary loss of stomatal bHLH developmental genes, including SPCH, MUTE, FAMA and SCRM2 orthologues, from the genome of the marine flowering plant eelgrass (*Zostera marina*) around 70–60 Ma ago correlates with a complete absence of stomata¹⁸.

Phylogenetic analyses indicate that homologues of FAMA-like genes of *Arabidopsis* are found in lineages that diverged early in the evolution of land plants¹⁹. Group Ia genes have not been identified in the liverwort *Marchantia polymorpha* or in algae, both plant lineages

lacking stomata, suggesting that Group Ia bHLHs are intimately linked to stomatal evolution. The *P. patens* genome harbours two Group Ia bHLH inparalogous genes, *PpSMF1* and *PpSMF2*^{6,19}, and four *SCRM1/SCRM2* Group 3b genes (*PpSCRM1*/Pp3c10_4260V3, Pp3c2_16410V3, Pp3c_20960V3 and Pp3c8_18070V3) (Figures 1 d,e). In line with a previous analysis with broader taxonomic sampling¹¹, our phylogenetic inference robustly suggests that *PpSMF1* and *PpSMF2* are co-orthologous to *AtFAMA* which, in *Arabidopsis*, is essential for guard cell fate. Both analyses robustly reject a (co-)orthologous relationship of the SMF genes in *Physcomitrella* and *Selaginella* with the MUTE/SPCH clade, as suggested by our earlier phylogenetic analysis⁶. Reasoning that genes encoding stomatal regulators would be preferentially expressed in the stomatal-bearing sporophyte, we interrogated microarray datasets²⁰ and *P. patens* transcriptome atlas results²¹ that identified *PpSMF1*, *PpSMF2* and *PpSCRM1* as strong candidates because of their up-regulation in the sporophyte relative to protonemal tissue, as supported by qRT-PCR (Figures 1 f–h; Supp. Info. Figures 1–2). Additionally, *PpSCRM1* is the most highly expressed of the four *PpSCRM* paralogues across *P. patens* tissues including developing sporophytes²¹ (Supp. Info. Figure 2). Based on these analyses, we investigated the role of *PpSMF1*, *PpSMF2* and *PpSCRM1* in regulating stomatal formation in *P. patens* by generating targeted gene deletion mutants via homologous recombination. Altogether, we generated two independent knock-out lines for each of *PpSMF1*, *PpSMF2*, and *PpSCRM1*. Flow cytometry analyses verified gametophytes of all the mutants were haploid, as in the wild-type, and not polyploid transformants (Supp. Info. Figure 3).

Stomata of *P. patens* form exclusively during the sporophyte stage of the life cycle (Figure 1a) and are restricted to a small area around the base (Figure 1b). *P. patens* lacks the early meristematic lineage for stomata seen in *A. thaliana*. Instead, the formation of a cell equivalent to a guard mother cell (GMC) is specified³ which, in common with the closely related *Funaria hygrometrica*²², appears to undergo an incomplete symmetric division leading to the formation of a single guard cell and a central pore (Figure 1c). Strikingly, in both *PpSMF1* and *PpSCRM1* mutant lines, the stomatal developmental program is halted resulting in no mature guard cells. Instead, only pavement-like cells develop and in *PpSCRM1*, very occasionally cells form that enter the stomatal lineage but fail to mature into stomata (Figures 2a, b). In contrast, *PpSMF2* mutants develop normal wild-type stomata (Figures 2a, b). We confirmed integration of the transgenes at the targeted loci and verified absence of gene expression in all mutant lines using genomic PCR and RT-PCR. (Figure 2c; Supp. Info. Figures 4–6). Closer anatomical inspection revealed a correlation between the presence of stomata and of sub-stomatal cavities, pointing to functional stomata: Sectioning of sporophytes revealed loss of stomata in *PpSMF1* and *PpSCRM1* was accompanied by the loss of sub-stomatal cavities, whereas in WT and in *PpSMF2* stomata and sub-stomatal cavities were present (Supp. Info. Figure 7). We found no differences in sporophyte sizes between the different mutants and WT lines (Supp. Info. Figure 8). These results establish *PpSMF1* and *PpSCRM1*, but not *PpSMF2*, as essential for the formation of stomata in *P. patens*. Our targeted knock-out results are independently supported by cross-species gene complementation studies in which *PpSMF1*, but not *PpSMF2*, partially complemented *A. thaliana* *mute* and *fama* mutants⁶. Taken together, these

data strengthen our hypothesis that a single ancestral *PpSMF1*-like gene and a *SCRM* partner were responsible for stomatal development in early land plants.

Because Group Ia bHLH proteins are obligate heterodimers with Group III bHLHs in *A. thaliana*, we next used bimolecular fluorescence complementation (BiFC) assays²³ and yeast two-hybrid (Y2H) experiments²⁴ to determine direct protein-protein interactions between PpSMF1 and PpSCRM1 *in vivo*. Transient co-expression of *PpSMF1::YFPn* and *PpSCRM1::YFPc*, as well as *PpSMF1::YFPc* and *PpSCRM1::YFPn*, resulted in strong YFP-fluorescence in the nuclei of *Allium cepa* cells, whereas no YFP-fluorescence was detected in controls (Figure 3a; Supp. Info. Figure 9). Specific interaction of PpSMF1 and PpSCRM1 was also demonstrated by Y2H experiments. PpSMF1 and PpSCRM1 fused with Gal4-DB alone showed no transcriptional activation, but strong activation was observed by using PpSMF1 as bait and PpSCRM1 as prey (Figures 3 b–d). These results support PpSMF1 and PpSCRM1 as physically-interacting heterodimeric partners. Furthermore, their nuclear localization is consistent with a role as DNA-binding transcription factors, reinforcing functional orthology to the *A. thaliana* Group Ia and IIIb bHLHs, respectively.

The BiFC and Y2H results suggest that PpSMF1-PpSCRM1 heterodimerisation could occur in *P. patens* cells due to highly conserved protein-protein interactions. *In-silico* analysis of the putative key domains involved in DNA binding during heterodimerisation suggests that an E-box binding domain (EBD) in PpSMF1 and PpSMF2, a corresponding DNA binding domain in PpSCRM1 and coiled-coil domains in both peptides are conserved between *P. patens* and *A. thaliana* (Supp. Info. Figure 10). However, *PpSMF2* expression is very low compared to *PpSMF1* and it is therefore unsurprising there is no aberrant phenotype in *PpSMF2* mutants despite key regulatory motifs being present. Conservation of functional motifs of PpSMF1 and PpSCRM1, which are both strongly expressed in the sporophyte²¹, taken together with our experimental data (Figures 1–3), suggests that a heterodimeric bHLH partnership first existed in the ancestor of mosses and flowering plants which could both initiate and complete stomatal development.

Having produced mosses with stomata-less sporophytes, we next addressed the long-standing mystery relating to stomatal function in an early diverging non-vascular land plant lineage^{5,25}. Current opinion suggests moss stomata facilitate nutrient and water transport and gas exchange in the developing sporophyte^{26,27} and also assist dehiscence and release of spores during sporophyte maturation²⁸, when pores become less able to close. We tested the function of stomata in *P. patens* in this context by tracking the development and subsequent dehiscence of the sporophytes in WT and mutants (Figure 4). Absence of stomata had no effect on spore development, morphology or viability in lines of *PpSMF1* and *PpSCRM1* as determined using SEM and bright-field microscopy and spore germination assays, respectively (Supp. Info. Figures 11 and 12). In contrast, observations of sporophyte development over time indicated that stomata-less *PpSMF1* and *PpSCRM1* mutants showed significantly ($P < 0.01$) delayed capsule dehiscence relative to WT during the late stages of development, as measured by the percentage of open capsules and timing of dehiscence (Figure 4; Supp. Info. Figures 13–14)., Although the reduced sporophyte of *Physcomitrella* is different to that of larger complex mosses, such as *Funaria*, our data suggest stomata during late stage sporophyte development may function in a similar manner

aiding capsule dehiscence²⁹. Intriguingly, delayed sporophyte dehiscence in *P. patens* seems to be decoupled from the browning of the sporophyte capsules, which is commonly assumed to be an indicator of capsule and spore maturation. As indicated by our quantitative analysis of the transition of capsule colouring (Supp. Info. Figure 15), *PpSMF1* capsules did not reveal any significant deviation from WT. However, in young green sporophytes of *P. patens*, and *F. hygrometrica*, stomata open and close in response to cues, such as light and abscisic acid, through molecular pathways co-opted from the gametophyte^{27,30}, suggesting gas exchange functionality. A complex picture of stomatal function in early land plant lineage sporophytes is therefore emerging relating to age, and possibly environmental conditions, but with stomatal action ultimately linked to reproductive success.

We propose that an ancestral land plant possessed a multifunctional ancestral dimer, comprised of ancient variants of PpSMF1 and PpSCRM1, which was sufficient to initiate and drive stomatal development in the early sporophyte. Specifically, results from our experiments with knock-out mutants in the moss *P. patens*, belonging to an extant lineage of non-vascular land plants with stomata, and our protein-protein interaction evidence, support the notion that a MUTE-FAMA-like and SCRM1/SCRM-like bHLH partnership was responsible for the origin of stomata in the earliest vascular land plants over 400 Ma. Remarkably, the origin of this genetic system that gave rise to stomata, together with those for roots^{10,11} and leafy shoots¹², ultimately helped facilitate the evolutionary radiation of plants on land leading to increases in terrestrial ecosystem complexity and primary production^{1,8,31} that supported a burgeoning diversity of life on the continents.

Methods

Plant material and culture conditions

Physcomitrella patens subspecies *patens* (Hedwig) Bruch & Schimp. WT strain “Gransden 2004”, used for genome sequencing³², provided the genetic background for the generation of *PpSCRM1* mutants (“Gransden 2004”, Freiburg) and ‘Villersexel’ the genetic background for the generation of *PpSMF1* mutants (Sheffield), and “Gransden D12” was the background for production of the *PpSMF2* mutants. *P. patens* was grown axenically on BCDAT medium³³ supplemented with 1 mM calcium chloride and overlaid with cellophane discs (AA Packaging, UK), in 9 cm Petri dishes sealed with Micropore tape (3M) in Sanyo MLR incubators under continuous light ($140 \mu\text{mol m}^{-2} \text{s}^{-1}$) at 25 °C³⁴. *P. patens* (Freiburg) was grown in liquid or on solid (12 g/L purified agar (OXOID, Thermo Scientific, Waltham, MA, USA)) supplemented Knop medium^{35,36} and cultivated at 23 °C under a 16-hour light and 8-hour dark cycle³⁷. Sporophyte development was induced according to ref³⁸.

Generation of transgenic lines

To create the PpSMF1 and PpSMF2 knock-out (KO) constructs for gene targeting, 5′- and 3′-targeting sequences (coordinates Chr22: 9308333-9307319 (5′) and Chr22: 9306131-9305111 (3′) for PpSMF1 and Chr19: 13226647-13227667 (5′) and Chr19: 13228404-13229099 (3′) for PpSMF2 were cloned on either side of a Kan^R(SMF1-KO) and Hyg^R (SMF2-KO) selection cassette, respectively. The resulting constructs were amplified by PCR and used to transform *P. patens*. To produce the *PpSCRM1* KO construct a 1,365 bp

fragment of the *PpSCRM1* gene (Pp3c10_4280) was PCR-amplified with the primers listed in Supp. Table 1 introducing EcoRI sites to the ends of the PCR product. After cloning to plasmid pJet1.2 (Thermo Fisher) an nptII selection cassette³⁹ was inserted into this fragment via unique restriction sites for HincII and BcuI, respectively. Before moss transformation the KO construct was released from the vector backbone via EcoRI digest. Polyethylene glycol-mediated protoplast transformation of *P. patens* and analysis and confirmation of gene targeted loci, were conducted according to ref (⁴⁰).

RNA was isolated from all tissues using the Spectrum Plant Total RNA Kit (Sigma-Aldrich) following the manufacturer's protocol. RNA was quantified using a NanoDrop ND-8000 UV-Vis spectrophotometer (ThermoScientific). For RT-PCR, eluted RNA was DNase-treated with Ambion DNA-free™ DNA Removal Kit and then used as a template for cDNA synthesis with M-MLV Reverse Transcriptase (Life Technologies, New York) as per the manufacturer's protocol. The resulting cDNA was used for PCR amplification (35 to 40 cycles) (Table S1 for primers). At the end of the PCR program samples were loaded into wells for agarose gel (1% w/v) electrophoresis and visualised by a UVitec (Cambridge, UK) digital camera. Primer sequences were designed and selected using Primer3 (<http://frodo.wi.mit.edu/primer3/>).

Molecular analysis

Three replicates of 7 day old protonemata grown on BCDAT, and 3 replicates of peat-pellet derived sporophyte capsules were used to compare the relative expression of PpSMF1, PpSMF2 and PpSCRM1. For protonemata, RNA was extracted from half a plate of tissue for each replicate. For sporophyte samples, early expanding sporophytes were harvested from 2 peat-pellets per replicate in order to generate sufficient RNA (approx. 300 capsules per replicate). RNA was extracted and processed using the above described methods. Prior to DNase treatment and cDNA synthesis the replicate RNA was assessed using the Nanodrop (Thermo Scientific) to ensure the same amount of RNA in all replicates prior to downstream applications. Relative qRT-PCR was performed using the Rotor-Gene SYBR Green PCR Kit (400) on a Corbett Rotor Gene 6000 (Qiagen, Venlo, Netherlands) following the manufacturer's protocols. Relative quantification was performed by normalising the take-off value and amplification efficiency of the genes analysed relative to three housekeeping genes⁴¹.

Microscopic analysis

For epidermal phenotyping, 5–7 mature sporophytes of each line, and the corresponding WT, were removed from individual peat pellet-grown gametophores beneath a Leica MZCFLIII stereomicroscope. Capsules were stored in a modified Carnoy's solution (2:1 ethanol: acetic acid) for a period of 2 weeks prior to dissection. Dissected sporophytes were viewed with an Olympus BX51 microscope and photomicrographs taken using an Olympus DD71 camera. Images were analysed using ImageJ software.

Sporophyte maturation and dehiscence

Gametophores were cultivated from spores on agar plates with Knop medium including microelements³⁶. Individual three week old colonies were identified and transferred to Knop

plates. Between 8 and 10 plants were isolated per plate and generating at least five plates per line. Plates were sealed with 7/8 of Parafilm and 1/8 of Micropore film and grown under long day conditions at 25 °C. After five weeks, plates were transferred into climate cabinets with short day conditions at 15 °C, sealed with Parafilm and grown for four weeks until formation of gametangia. Fertilization was initialized by soaking plates with sterilised water (re-closed with Parafilm), re-opening the plates after five days to remove the water, resealing with Micropore film and then cultured for three to six weeks at 15 °C short-day conditions. Developing sporophytes were recorded and traced by marking and numbering them on the plate lids as they appeared.

Supplementary Material

Refer to Web version on PubMed Central for supplementary material.

Acknowledgments

We thank Richard Haas and Tim Fulton for excellent technical assistance. R.C. was supported by a NERC studentship. D.C.B is a GBMF investigator of the Howard Hughes Medical Institute. D.J.B. acknowledges funding through an ERC Advanced Grant (CDREG, 322998). R.R. acknowledges funding through the Excellence Initiative of the German Federal and States Governments (EXC294). A.C.C. and Y.K. acknowledge support from BBSRC (Grant numbers BB/F001797/1 and BB/1006710/1).

References

- Berry JA, Beerling DJ, Franks PJ. Stomata: key players in the earth system, past and present. *Current Opinion in Plant Biology*. 2010; 13:233–240. DOI: 10.1016/j.pbi.2010.04.013 [PubMed: 20552724]
- Chater C, Gray JE, Beerling DJ. Early evolutionary acquisition of stomatal control and development gene signalling networks. *Current Opinion in Plant Biology*. 2013; 16:638–646. DOI: 10.1016/j.pbi.2013.06.013 [PubMed: 23871687]
- Vaten A, Bergmann DC. Mechanisms of stomatal development: an evolutionary view. *Evodevo*. 2012; 3:9. [PubMed: 22512981]
- Pressel S, Goral T, Duckett JG. Stomatal differentiation and abnormal stomata in hornworts. *Journal of Bryology*. 2014; 36:87–103. DOI: 10.1179/1743282014y.0000000103
- Haberlandt, G. *Physiologische Pflanzenanatomie*. 5. Engelmann; 1918.
- MacAlister CA, Bergmann DC. Sequence and function of basic helix-loop-helix proteins required for stomatal development in Arabidopsis are deeply conserved in land plants. *Evolution & Development*. 2011; 13:182–192. DOI: 10.1111/j.1525-142X.2011.00468.x [PubMed: 21410874]
- Kanaoka MM, et al. SCREAM/ICE1 and SCREAM2 specify three cell-state transitional steps leading to Arabidopsis stomatal differentiation. *Plant Cell*. 2008; 20:1775–1785. DOI: 10.1105/tpc.108.060848 [PubMed: 18641265]
- Beerling, DJ. *The emerald planet: how plants changed Earth's history*. Oxford University Press; 2007.
- Edwards D, Kerp H, Hass H. Stomata in early land plants: an anatomical and ecophysiological approach. *Journal of Experimental Botany*. 1998; 49:255–278. DOI: 10.1093/jexbot/49.suppl_1.255
- Menand B, et al. An ancient mechanism controls the development of cells with a rooting function in land plants. *Science*. 2007; 316:1477–1480. DOI: 10.1126/science.1142618 [PubMed: 17556585]
- Tam THY, Catarino B, Dolan L. Conserved regulatory mechanism controls the development of cells with rooting functions in land plants. *Proceedings of the National Academy of Sciences of the United States of America*. 2015; 112:E3959–E3968. DOI: 10.1073/pnas.1416324112 [PubMed: 26150509]

12. Harrison CJ, et al. Independent recruitment of a conserved developmental mechanism during leaf evolution. *Nature*. 2005; 434:509–514. DOI: 10.1038/nature03410 [PubMed: 15791256]
13. Sakakibara K, Nishiyama T, Deguchi H, Hasebe M. Class 1 KNOX genes are not involved in shoot development in the moss *Physcomitrella patens* but do function in sporophyte development. *Evolution & Development*. 2008; 10:555–566. DOI: 10.1111/j.1525-142X.2008.00271.x [PubMed: 18803774]
14. Horst NA, et al. A single homeobox gene triggers phase transition, embryogenesis and asexual reproduction. *Nature Plants*. 2016; 2:6.
15. Raven JA. Selection pressures on stomatal evolution. *New Phytologist*. 2002; 153:371–386. DOI: 10.1046/j.0028-646X.2001.00334.x
16. MacAlister CA, Ohashi-Ito K, Bergmann DC. Transcription factor control of asymmetric cell divisions that establish the stomatal lineage. *Nature*. 2007; 445:537–540. DOI: 10.1038/nature05491 [PubMed: 17183265]
17. Chinnusamy V, et al. ICE1: a regulator of cold-induced transcriptome and freezing tolerance in *Arabidopsis*. *Genes & Development*. 2003; 17:1043–1054. DOI: 10.1101/gad.1077503 [PubMed: 12672693]
18. Olsen JL, et al. The genome of the seagrass *Zostera marina* reveals angiosperm adaptation to the sea. *Nature*. 2016; 530:331–+. DOI: 10.1038/nature16548 [PubMed: 26814964]
19. Ran JH, Shen TT, Liu WJ, Wang XQ. Evolution of the bHLH Genes Involved in Stomatal Development: Implications for the Expansion of Developmental Complexity of Stomata in Land Plants. *Plos One*. 2013; 8:11.
20. O'Donoghue MT, et al. Genome-wide transcriptomic analysis of the sporophyte of the moss *Physcomitrella patens*. *Journal of Experimental Botany*. 2013; 64:3567–3581. DOI: 10.1093/jxb/ert190 [PubMed: 23888066]
21. Ortiz-Ramirez C, et al. A Transcriptome Atlas of *Physcomitrella patens* Provides Insights into the Evolution and Development of Land Plants. *Mol Plant*. 2016; 9:205–220. DOI: 10.1016/j.molp.2015.12.002 [PubMed: 26687813]
22. Sack FD, Paolillo DJ. Incomplete cytokinesis in *Funaria* stomata. *American Journal of Botany*. 1985; 72:1325–1333. DOI: 10.2307/2443504
23. Weinthal D, Tzfira T. Imaging protein-protein interactions in plant cells by bimolecular fluorescence complementation assay. *Trends in Plant Science*. 2009; 14:59–63. DOI: 10.1016/j.tplants.2008.11.002 [PubMed: 19150604]
24. Ito T, et al. A comprehensive two-hybrid analysis to explore the yeast protein interactome. *Proc Natl Acad Sci U S A*. 2001; 98:4569–4574. DOI: 10.1073/pnas.061034498 [PubMed: 11283351]
25. Haig D. Filial mistletoes: the functional morphology of moss sporophytes. *Annals of Botany*. 2013; 111:337–345. DOI: 10.1093/aob/mcs295 [PubMed: 23277472]
26. Merced A, Renzaglia KS. Moss stomata in highly elaborated *Oedipodium* (*Oedipodiaceae*) and highly reduced *Ephemerum* (*Pottiaceae*) sporophytes are remarkably similar. *American Journal of Botany*. 2013; 100:2318–2327. DOI: 10.3732/ajb.1300214 [PubMed: 24302694]
27. Chater C, et al. Regulatory Mechanism Controlling Stomatal Behavior Conserved across 400 Million Years of Land Plant Evolution. *Current Biology*. 2011; 21:1025–1029. DOI: 10.1016/j.cub.2011.04.032 [PubMed: 21658944]
28. Garner DLB, Paolillo DJJ. On the functioning of stomates in *Funaria*. *Bryologist*. 1973; 76:423–427. DOI: 10.2307/3241726
29. Merced A, Renzaglia KS. Patterning of stomata in the moss *Funaria*: a simple way to space guard cells. *Annals of Botany*. 2016; 117:985–994. DOI: 10.1093/aob/mcw029 [PubMed: 27107413]
30. Lind C, et al. Stomatal Guard Cells Co-opted an Ancient ABA-Dependent Desiccation Survival System to Regulate Stomatal Closure. *Current Biology*. 2015; 25:928–935. DOI: 10.1016/j.cub.2015.01.067 [PubMed: 25802151]
31. Franks PJ, Beerling DJ. Maximum leaf conductance driven by CO₂ effects on stomatal size and density over geologic time. *Proceedings of the National Academy of Sciences of the United States of America*. 2009; 106:10343–10347. DOI: 10.1073/pnas.0904209106 [PubMed: 19506250]
32. Rensing SA, et al. The *Physcomitrella* genome reveals evolutionary insights into the conquest of land by plants. *Science*. 2008; 319:64–69. DOI: 10.1126/science.1150646 [PubMed: 18079367]

33. Cove D. The moss, *Physcomitrella patens*. *Journal of Plant Growth Regulation*. 2000; 19:275–283. DOI: 10.1007/s003440000031
34. Wallace S, et al. Conservation of Male Sterility 2 function during spore and pollen wall development supports an evolutionarily early recruitment of a core component in the sporopollenin biosynthetic pathway. *New Phytologist*. 2015; 205:390–401. DOI: 10.1111/nph.13012 [PubMed: 25195943]
35. Reski R, Abel WO. Induction of budding on chloronemata and caulonemata of the moss, *Physcomitrella patens*, using isopenentenyladenine. *Planta*. 1985; 165:354–358. DOI: 10.1007/bf00392232 [PubMed: 24241140]
36. Egener T, et al. High frequency of phenotypic deviations in *Physcomitrella patens* plants transformed with a gene-disruption library. *BMC plant biology*. 2002; 2:6. [PubMed: 12123528]
37. Frank W, Ratnadewi D, Reski R. *Physcomitrella patens* is highly tolerant against drought, salt and osmotic stress. *Planta*. 2005; 220:384–394. DOI: 10.1007/s00425-004-1351-1 [PubMed: 15322883]
38. Hohe A, Rensing SA, Mildner M, Lang D, Reski R. Day length and temperature strongly influence sexual reproduction and expression of a novel MADS-box gene in the moss *Physcomitrella patens*. *Plant Biology*. 2002; 4:595–602. DOI: 10.1055/s-2002-35440
39. Hohe A, et al. An improved and highly standardised transformation procedure allows efficient production of single and multiple targeted gene-knockouts in a moss, *Physcomitrella patens*. *Curr Genet*. 2004; 44:339–347. DOI: 10.1007/s00294-003-0458-4 [PubMed: 14586556]
40. Kamisugi Y, Cuming AC, Cove DJ. Parameters determining the efficiency of gene targeting in the moss *Physcomitrella patens*. *Nucleic Acids Research*. 2005; 33:10.
41. Luna E, et al. Plant perception of beta-aminobutyric acid is mediated by an aspartyl-tRNA synthetase. *Nature Chemical Biology*. 2014; 10:450–456. DOI: 10.1038/nchembio.1520 [PubMed: 24776930]

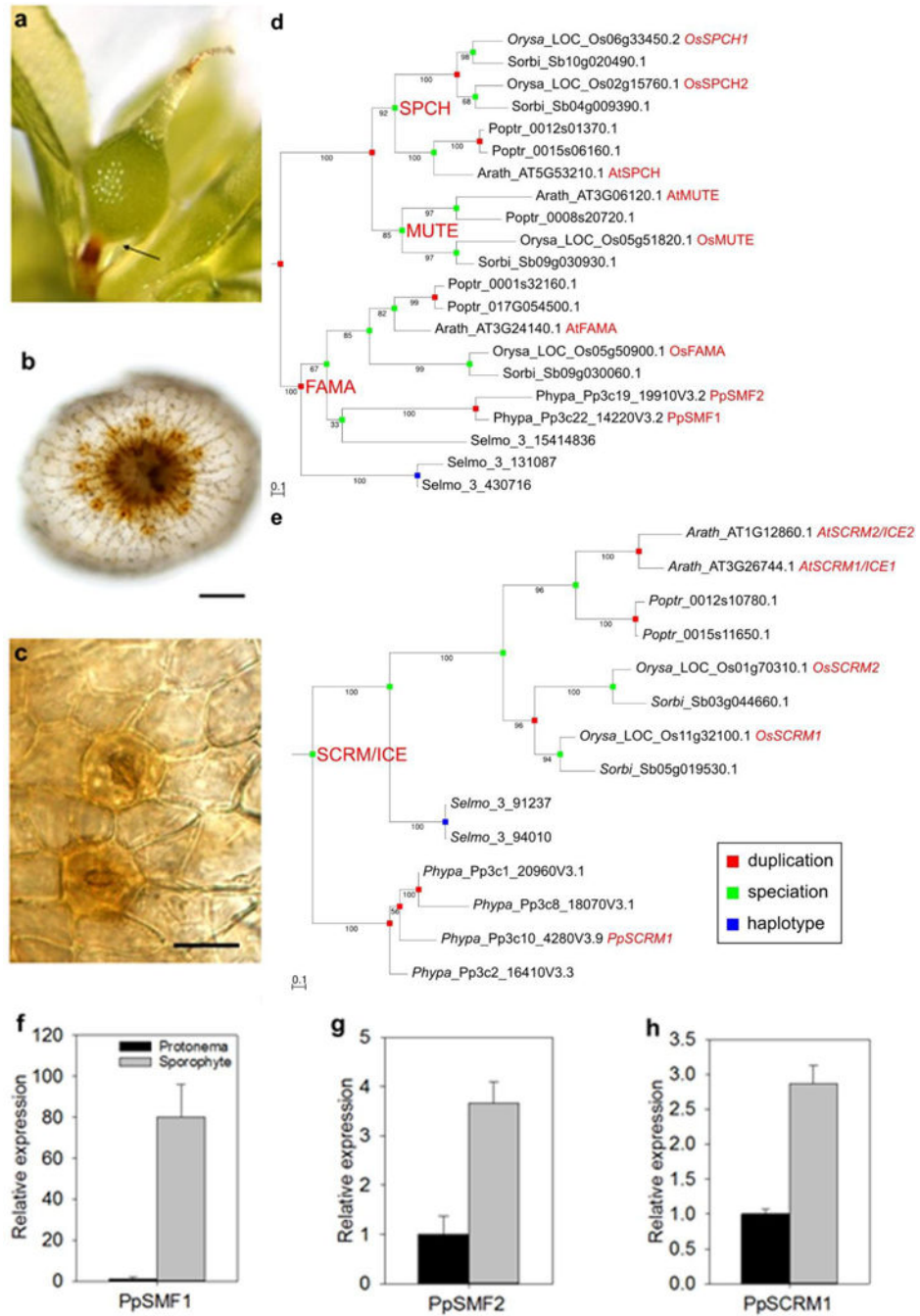


Figure 1. The moss *Physcomitrella patens* genome encodes orthologues of the basic helix loop helix (bHLH) transcription factors regulating stomatal development in flowering plants (a) Developing *P. patens* sporophyte, arrow indicating region of stomatal placement, and (b) excised sporophyte with stomata (orange/brown pores) forming a ring around the base. (c) Close-up of the sporophyte epidermis with single celled guard cells and central pores. (d and e) Bootstrapped Maximum Likelihood phylogenies of the SMF gene family comprising the FAMA, SPCH and MUTE subfamilies and the SCRM/ICE gene family in sequenced land plants. Internal node names in bold red indicate inferred subfamily ancestry. Internal nodes are coloured to indicate either duplication (red), speciation (green) or haplotype (blue) origin

of the descendant nodes. Edge values represent bootstrap values. External node names comprise species abbreviations, original accession numbers of the protein sequences and accepted gene names of experimentally studied representatives in bold red. Species abbreviations in five-letter-code: *Arabidopsis thaliana*, *Populus trichocarpa*, *Oryza sativa*, *Sorghum bicolor*, *Selaginella moellendorffii* and *Physcomitrella patens*. (f, g and h) Relative expression of *PpSMF1*, *PpSMF2* and *PpSCRM1* in the developing sporophyte (grey bars) and protonema tissue (black bars) analysed by qRT-PCR. Error bars indicate standard error of the mean. Three replicates per tissue type were used. The scale bar in **a** = 100µm, in **b** = 100µm, in **c** = 25µm.

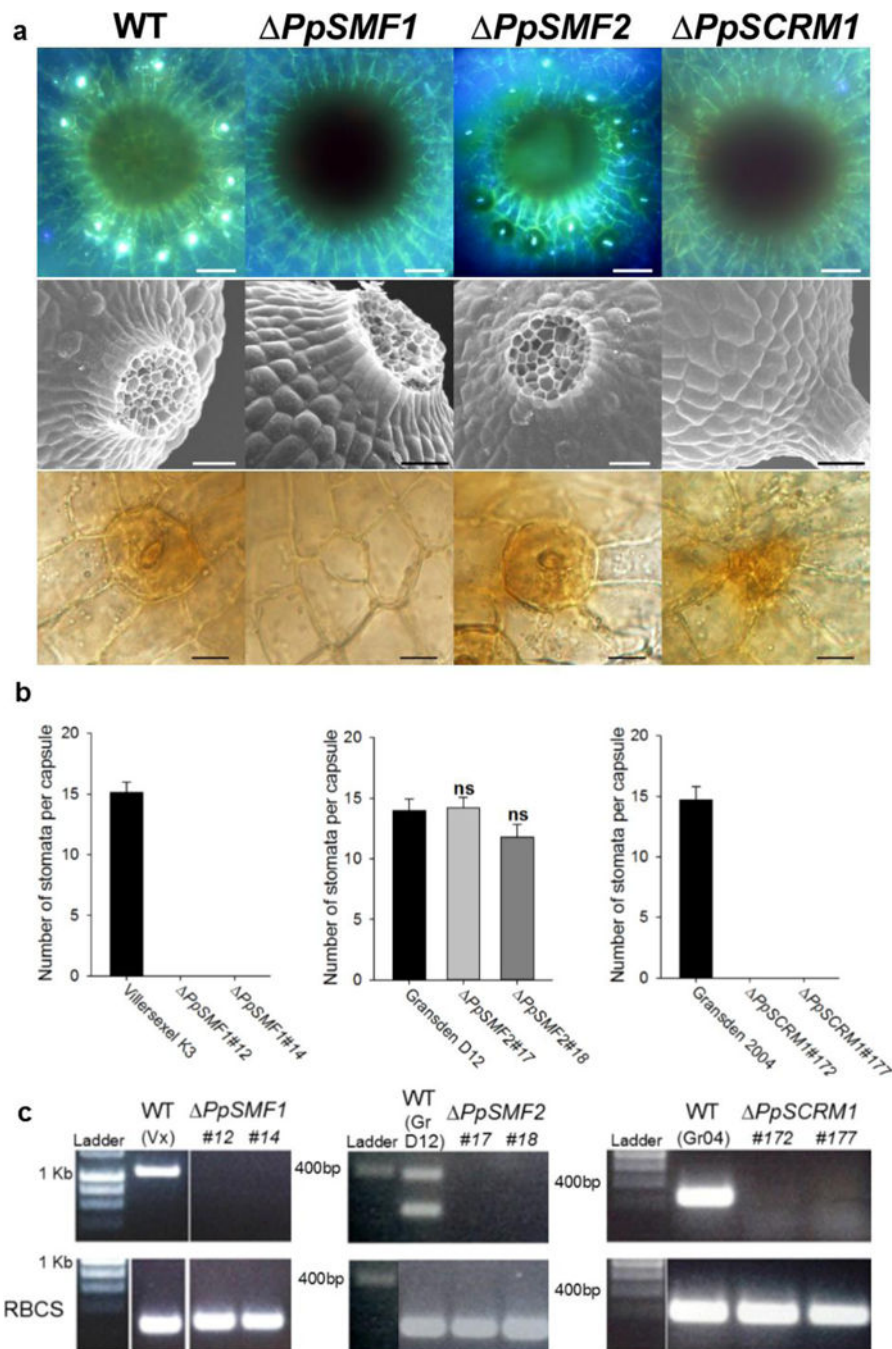


Figure 2. PpSMF1 and PpSCRM1 are required for stomatal development in the moss *Physcomitrella patens*

(a) Stacked UV fluorescence images (upper panel), scanning electron microscope images (middle panel) and bright field images (bottom panel) showing the spore capsule base and epidermal close-ups from *P. patens* wild-type, *PpSMF1*, *PpSMF2* and *PpSCRM1* knock-out mutants, respectively. The top panel wild-type representative is from Villersexel K3 ecotype of *P. patens*, the middle panel wild-type representative is from the Gransden D12 ecotype and the bottom panel wild-type relates to the Gransden 2004 ecotype. There were no

discernible differences between the sporophytes of the different background lines. For both of the *PpSCRM1* lines generated we observed one such instance of aborted stomata (see bottom right panel) in the 7 capsules of each line surveyed. **(b)** Number of stomata formed per sporophyte in two independent lines of each genotype versus wild-type controls. Error bars indicate one standard error of the mean. For *PpSMF1* and *PpSCRM1* and the corresponding wild-types, $n = 7$ capsules of each line were analysed. For *PpSMF2* and wild-type background, 5 capsules were surveyed. A One-way ANOVA was performed to test for differences between the wild-type and *PpSMF2* lines and no significant differences (denoted ns) were found. **(c)** RT-PCR to confirm loss of the respective transcript in each of the *P. patens* knock-out lines (top panel). A Rubisco (RBCS) control was run to verify the integrity of the produced cDNA (Bottom panel). For labelling purposes the wild-types Villersexel K3, Gransden D12 and Gransden 2004 are denoted Vx, GrD12 and Gr04. For *PpSMF2* two bands were amplified in the control for which the smaller 239bp product represents the size expected for *PpSMF2*. Scale bars in **a** = 50 μm in the top and middle panels, in the bottom panel = 15 μm .

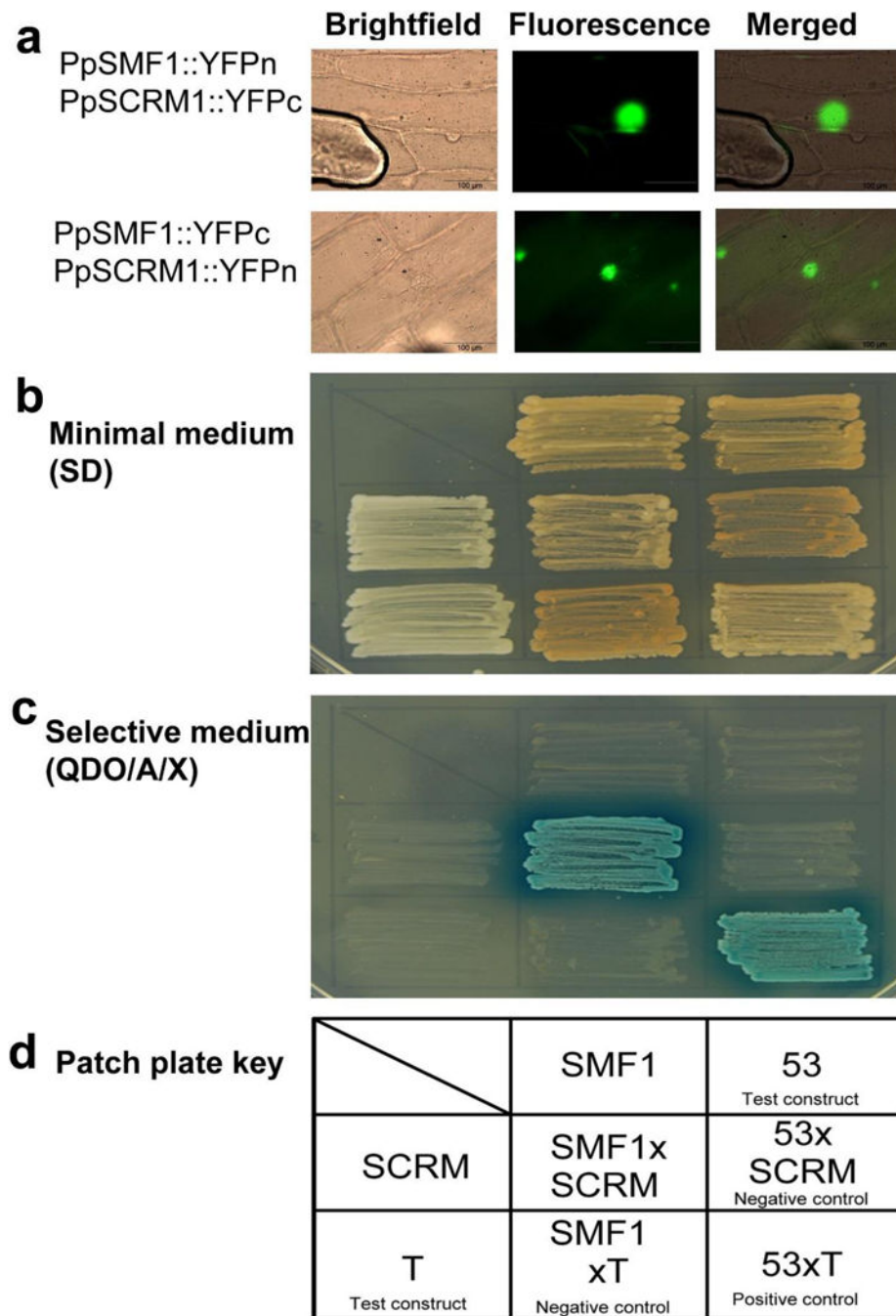


Figure 3. Bimolecular fluorescence complementation and Yeast 2-Hybrid assays demonstrating PpSMF1 and PpSCRM1 protein-protein interactions

(a) Representative bright-field, fluorescence and overlay/merged images of BiFC analysis showing pairwise combinations of bHLH constructs, each fused with a complementary, half-YFP molecule (nYFPn fusion and YFPc fusions, respectively). In the intact *Allium cepa* epidermis using bimolecular fluorescent complementation (BiFC), PpSMF1 and PpSCRM1 showed strong heterodimerization in the nuclei. Controls are described in Supp. Info. Fig 9. Scale = 100 μ m. (b–d) Yeast two-hybrid analysis: (b) Growth on minimal medium. (c)

Growth on stringent selection medium. Blue indicates reporter activation. **(d)** Key to patch plate assays is shown in (b) and (c).

Author Manuscript

Author Manuscript

Author Manuscript

Author Manuscript

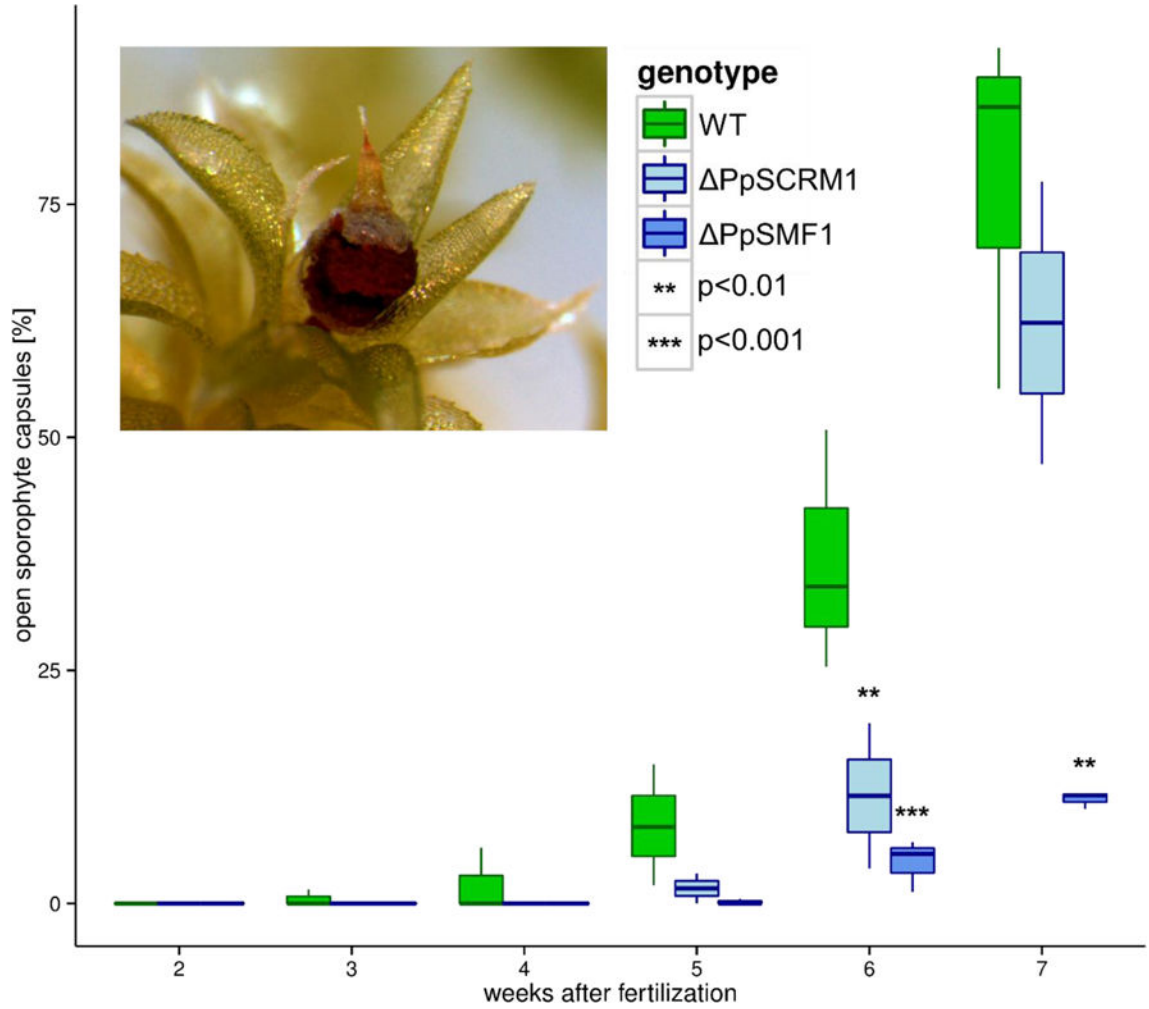


Figure 4. Loss of PpSMF1 and the PpSCRM1 gene functions results in delayed dehiscence of spore capsules

Box-whisker plots of the percentages of ruptured sporophyte capsules in the wild-type, PpSMF1 and PpSCRM1 lines over a developmental time series experiment ranging from second and seventh week after induction of fertilization. Vertical lines within boxes mark the median. The boxes indicate the upper (75 %) and lower (25 %) quartiles. Whiskers indicate the ranges of the minimal and maximal values. Inset photograph depicts an open/ruptured spore capsule in the Gransden wild-type strain. Significance of differences between mutants and the wild type was tested using a binomial model with a nested error term correcting for repeated measurements in the combined data set, and for each genetic background independently, with consistent results. Significant ($P < 0.05$) deviations from the wild type are indicated by asterisks.